Features of single tracks in coaxial laser cladding of a NI-based self-fluxing alloy

Eugene Feldshtein[1,*], *Oleg* Devojno[2], *Marharyta* Kardapolava[2] and *Nikolaj* Lutsko[2]

[1] Faculty of Mechanical Engineering, University of Zielona Góra, Prof. Z. Szafrana 4, 65-516 Zielona Góra, Poland
[2] Faculty of Mechanical Engineering, Belarusian National Technical University, Khmelnitsky str., 9, build. 6, Minsk 220013, Belarus

Abstract. In the present paper, the influence of coaxial laser cladding conditions on the dimensions, microstructure, phases and microhardness of Ni-based self-fluxing alloy single tracks is studied. The height and width of single tracks depend on the speed and distance of the laser cladding: increasing the nozzle distance from the deposited surface 1.4 times reduces the width of the track 1.2 – 1.3 times and increases its height 1.2 times. The increase of the laser spot speed 3 times reduces the track width 1.2 – 1.4 times and the height in 1.5 – 1.6 times. At the same time, the increase of the laser spot speed 3 times reduces the track width 1.2 – 1.4 times and the height 1.5 – 1.6 times. Regularities in the formation of single tracks microstructure with different cladding conditions are defined, as well as regularity of distribution of elements over the track depth and in the transient zone. The patterns of microhardness distribution over the track depth for different cladding conditions are found.

1 Introduction

Laser cladding (LC) is one of efficient methods to deposit on machine parts different coatings including functionally graded, multilayered, etc. It is possible to mix different powders while injecting them into a cladding zone and produce coatings with desired content, to create engineered internal structures [1–3].

Several groups can be identified among the factors affected laser cladding [4–10]. These groups include the following:

- a dependence on laser radiation conditions (laser power, pulse energy, pulse duration, pulse frequency, laser wave length, laser beam spot diameter, focal distance),
- a dependence on conditions of layer forming (laser scan speed, scan strategy rotation, number of spots, scanning space, stripe width, stripe overlap, hatch or track distance, layer thickness, gas content control),
- a dependence on characteristics of powders that was used (size of the powder particles, powder mass flow, temperature of the powder).

A number of studies have been carried out to investigate the properties of single tracks when laser cladding. In particular, in [11] the relationships between geometrical characteristics (width, height, area, and penetration depth) and the processing parameters (laser power, scanning speed and powder mass flow) for 316L stainless steel single tracks were discussed. In [12] the surface morphology and microstructure of single tracks and layer of this steel after introduction of a NiB additive were described. The microstructure and porosity evaluation in single tracks of the Ni60 self-fluxing alloy deposited by laser-cladding technique are discussed in [13]. The microstructure and nano-mechanical properties of single tracks and layer of AlSi10Mg alloy after SLM were researched in [14], and the density, roughness and microstructure of AlSi10Mg layer were described in [15]. The microstructural and mechanical properties and surface quality of CoCrMo alloy and their relationship with some of the cladding parameters were studied in [8,16] for single tracks and the surface.

In the latter case, different coating materials can be used, and self-fluxing alloys are widely applied among them. Three groups of these alloys are known now: Fe-based, Ni-based, and Co-based self-fluxing alloys [13,17–22]. The Ni- and Co-based self-fluxing alloys are characterized by wettability, deoxidization and by a fluxing effect as well as high physical and mechanical properties, and a good resistance to wear, oxidation and high temperature corrosion. The multiphase structure that is formed in the layer of Ni-based self-fluxing alloy during the reflow process ensures a high wear resistance of such coatings. It was reported in the above-mentioned research studies that carbides, chromium borides, a solid solution, and a eutectic phase are the constituents of the coating. It was also reported that chromium-molybdenum carbides and chromium-molybdenum borides, nickel borides, chromium carbides and borides were present in the nickel matrix of the coating.

The aim of the present investigation is to study the formation features, microstructure and chemical composition and microhardness of single laser tracks of a NiCrBSi self-fluxing coatings.

* Corresponding author: E.Feldsztein@ibem.uz.zgora.pl

2 Experimental procedures

2.1 Material

The research was carried out with NiCrBSi self-fluxing hard alloy. The chemical composition of the powder is: 0.3–0.6 % C, 1.7–2.5 % B, 1.2–3.2 % Si, 8–14 % Cr, 1.2–1.3 % Fe and Ni is the rest. The hardness of the material is equal HRC 35–40.

2.2 Laser cladding technology

The single tracks were applied to a substrate of AISI 1045 steel. Cladding was performed using a continuous-wave CO_2 laser "Comet 2" with the power of 1 kW (Fig. 1). Powder was fed to the work area through a lens with a nozzle for spot coaxial laser cladding. The compressed air was used as a transporting gas. The focal length was of 200 mm, and a focused spot was of 1.0 mm.

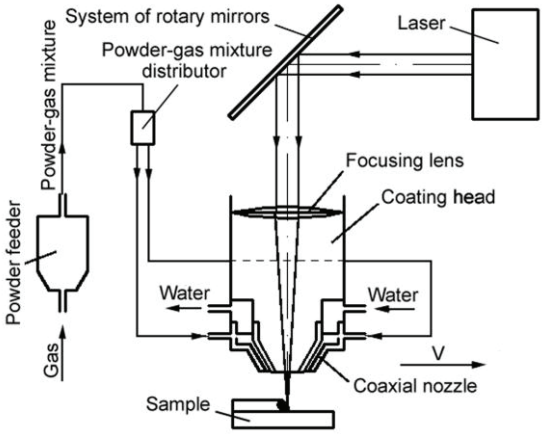

Fig. 1. The scheme of a single track deposition.

2.3 Preparation of samples

Cladding tracks of the Ni-based alloy were tested in the speed range of 40–120 mm/min when the distance between the nozzle and the surface of sample was of 10–14 mm. The diameter of the laser spot was of 1 mm, which corresponds to a power density of $1.27 \cdot 10^5$ W/cm^2. After cladding the samples were cut in the direction perpendicular to the tracks, and then their transverse metallographic sections were made and the geometric parameters of the single track, i.e., width B and height H, were determined.

2.4 Measuring equipment

The track sizes were measured using an optical microscope with accuracy of 0.001 mm. The microstructure, morphology and chemical composition were analyzed by a scanning electron microscope "Mira". The microhardness was measured using a MICROMET II Hardness Tester. Statistica 12 software was used for a graphical interpretation of some results.

3. Results and discussion

3.1 Influence of laser cladding conditions on the single track geometry

The effect of laser cladding conditions on the height H and width B of single tracks is shown in Fig. 2. It can be seen that increasing the nozzle distance from the deposited surface 1.4 times reduces the width of the track 1.2 – 1.3 times and increases its height 1.2 times. At the same time, the increase of the laser spot speed 3 times reduces the track width 1.2 – 1.4 times and the height 1.5 – 1.6 times.

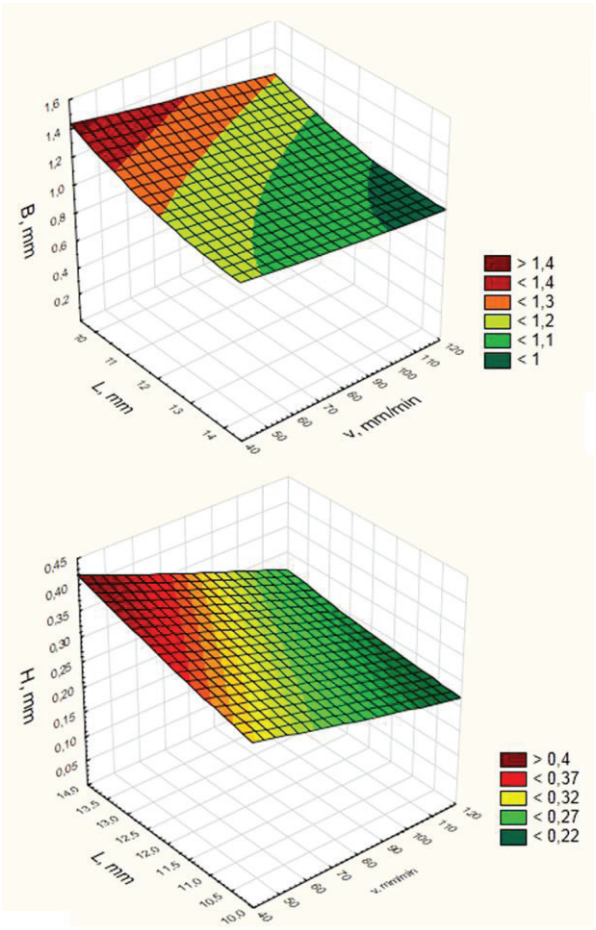

Fig. 2. The dependence of the track dimensions on the deposition speed v and the distance L between the nozzle and the sample surface.

3.2 Microstructure and phase composition of single tracks

Studies of the single track structure have shown that the deposited tracks have a dense composition with distinct structural components and consist of three regions (Fig. 3): the deposited material (1), heat affected zone (2) and the base material (3).
The structure of the deposited track consists of γ-Ni (Ni-based solid solution) as well as chromium borides and carbides.

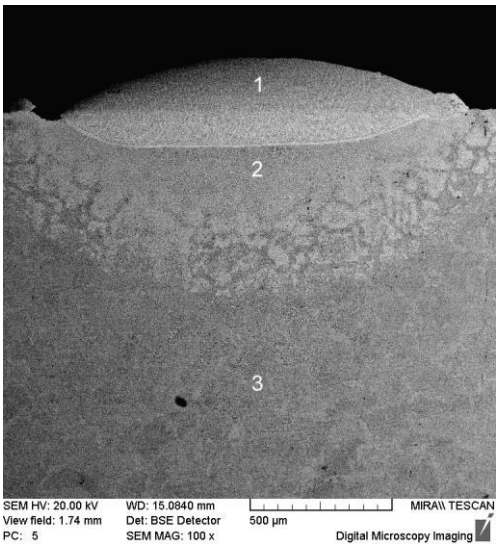

Fig. 3. The microstructure of a single track and the heat affected zone.

The structure is formed under the influence of high temperatures, high cooling speed and directional heat removal. Dendrites of the first and second orders are seen in the upper region of the deposited layer and they are arranged at an angle of 45° to the surface. The self-fluxing alloy powder is melted at high temperatures and crystallized in the pseudo-dendrites form and complex quasi-eutectic γ-Ni + Ni_3B is formed between dendrite branches at temperatures 950 – 1000 °C. First-order branches of dendrites are crystallized in the first place and they contain the maximum amount of the powder constituent elements. The branches of the second and third orders contain a reduced amount of reinforcing components. The lower the rate of deposition, the more slowly a eutectic mixture is crystallized. This mixture is characterized by the ability to cure the pores and moreover it reduces the possibility of cracking. The lower part of the deposited layer is at high temperatures a long time and the dendrite-globular structure with a eutectic mixture of γ-Ni + Ni_3B is formed there. The heat affected zone is formed between the deposited single track and the substrate material and the thickness of it is equal to 10 – 40 µm. Its presence indicates the chemical interaction between the coating material and the substrate. During contact between double surfaces the restoration of metal oxide films is observed due to the presence of strong oxidants: boron and silicon. The formed borosilicate glass floats to the surface of the coating or evaporates. The bimetal bond strength becomes equal to the strength of the substrate metal in this case but with increasing residence times in the liquid pond the interdiffusion of iron and nickel and a significant decrease in hardness can be observed. Structures of tempered martensite and troostite are formed in the upper region of the heat affected zone under high temperatures. Directly at the interface the temperature effect is insufficient for dissolution of the grain boundaries, but quenching and tempering processes occur inside grains.

3.3 The distribution of elements over the depth of single tracks

The analysis of the elements distribution over the depth of PG-12H-01 alloy single track showed that at a depth of 0.1 mm below the coating, i.e. in the substrate material, almost pure iron is present and the content of other elements is close to zero (Fig. 4). At the boundary of the coating and substrate, i.e. in the transient zone, the iron content is reduced to 65 %, the nickel content is increased to 27 % and chromium up to 6 %. Thus, an active mixing of the coating and substrate materials takes place in the molten pond. Further away from the substrate material surface, the content of elements practically does not change, but does not reach the values typical for the in-situ powder. The reason for this discrepancy is the strong mixing of the substrate and coating materials when a single track is formed.

Features of mixing and interaction of the coating and substrate materials in the transient zone of the single track are shown in Fig. 5. At a depth of more than 5 µm under the coating the material composition consists of practically pure iron, whereas at the boundary between the coating and the substrate material the composition is: 79 % iron, 17 % nickel, 4 % chromium and 1 % silicon, indicating that an active interaction of materials takes place. Further, the material composition of the deposited track practically does not change throughout the depth of the transient zone, and its thickness is negligible. The fact that the material composition in the transient zone of the single track is almost the same as throughout the coating depth is caused by strong mixing of the coating and substrate material.

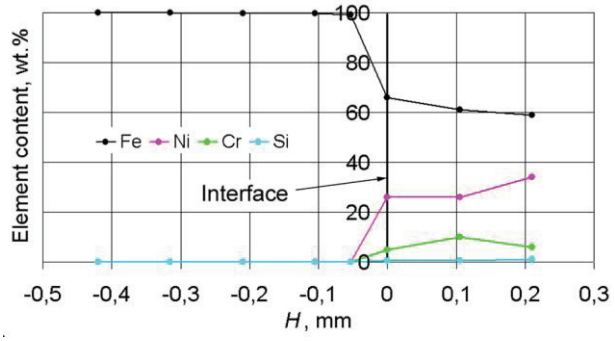

Fig. 4. The distribution of elements at a depth of a single track.

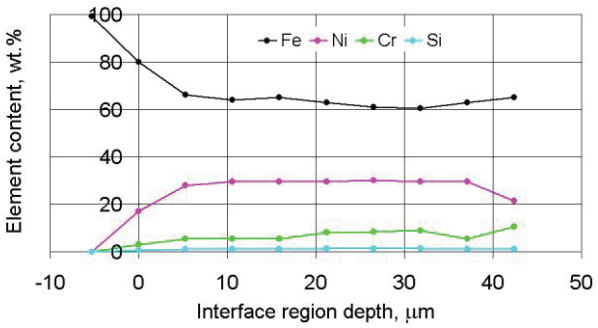

Fig. 5. The distribution of elements in the transient zone of a single track.

3.4 Microhardness of single tracks

Changes of the microhardness in the depth of single tracks for various cladding conditions are shown in Fig. 6. Based on the measurements made, the following can be noted:

- microhardness near the track surface is not high (150 – 500 HV100), then its growth is observed, and then its gradual reduction to the microhardness of the substrate;
- lowest microhardness (120 – 150 HV100) is observed at the cladding speed of 40 mm/min for all cladding distances;
- when the cladding speed increases up to 100 mm/min, an increase of microhardness up to 500 – 650 HV100 is observed, but the cladding speed of 120 mm/min decreases the microhardness again to a value, which was observed at the cladding speed of 80 mm/min (300 – 350 HV100);
- some increase in the microhardness is observed with decreasing the cladding distance;
- the highest microhardness (700 HV100) is observed at the cladding speed of 100 mm/min and a cladding distance of 10 mm;
- at low deposition rates, less than 60 mm/min, the overall level of microhardness is low and equals 150 – 350 HV100.

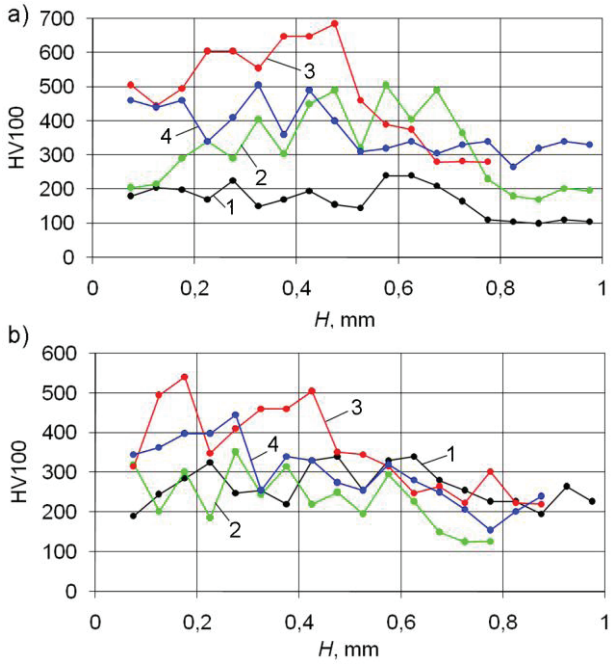

Fig. 6. Microhardness changes in the single track depth for the distance from the nozzle to the sample surface of 10 mm (a) and 14 mm (b): 1 – v = 40 mm/min, 2 – v = 80 mm/min, 3 – v = 100 mm / min, 4 – v = 120 mm/min.

4 Conclusions

The novelty of this investigation is the complex analysis of single tracks of an Ni-based self-fluxing alloy that have been formed by laser cladding using the CW CO_2 laser. The height and width of single tracks depend on the speed and distance of the laser cladding: increasing the nozzle distance from the deposited surface 1.4 times reduces the width of the track 1.2 – 1.3 times and increases its height 1.2 times. The increase of the laser spot speed 3 times reduces the track width 1.2 – 1.4 times and the height in 1.5 – 1.6 times. At the same time, the increase of the laser spot speed 3 times reduces the track width 1.2 – 1.4 times and the height 1.5 – 1.6 times. Regularities in the formation of single tracks microstructure with different cladding conditions are defined, as well as regularity of distribution of elements over the track depth and in the transient zone. The patterns of microhardness distribution over the track depth for different cladding conditions are found. On the basis of the investigated features of the single tracks formation, it is possible to provide a quality coating as a whole. On the basis of the investigated features of the single tracks formation, it is possible to provide a quality coating as a whole.

References

1. J.C. Ion, *Laser Processing of Engineering Materials. Principles, Procedure and Industrial Application* (Elsevier Ltd., Oxford, 2005)
2. W.M. Steen, *Laser Material Processing* (Springer, 2003)
3. E. Toyserkani, A. Khajepour, S. Corbin, *Laser Cladding* (CRS Press, 2005)
4. D. Dimitrov, K. Schreve, N.D. Beer, Rapid Prototyp. J. **12** (2006)
5. I. Yadroitsev, P. Bertrand, I. Smurov, Appl. Surf. Sci. **253** (2007)
6. J. Ciurana, L. Hernandez, J. Delgado, Int. J. Adv. Manuf. Technol. **68** (2013)
7. M. Averyanova, E. Cicala, P. Bertrand, D. Grevey, Rapid Prototyp. J. **18** (2012)
8. Y. Pupo, K.P. Monroy, J. Ciurana. Int. J. Adv. Manuf. Technol. **80** (2015)
9. L.E. Criales, Y.M. Arısoy, B. Lane, S. Moylan, A. Donmez, T. Özel, Add. Manuf. **13** (2017)
10. A.J. Dunbar, E.R. Denlinger, J. Heigel, P. Michaleris, P. Guerrier, R. Martukanitz, T.W. Simpson, Add. Manuf. **12** (2016)
11. H. El Cheikh, B. Courant, S. Branchu, J.-Y. Hascoët, R. Guillén, Opt. Lasers Eng. **50** (2012)
12. J. Stašić, D. Božić, Surf. Coat. Technol. **307** (2016)
13. C. Zeng, W. Tian, W.H. Liao, L. Hua, Surf. Coat. Technol. **294** (2016)
14. N.T. Aboulkhair, I. Maskery, C. Tuck, I. Ashcroft, N.M. Everitt, J. Mater. Proc. Technol. **230** (2016)
15. K. Kempen, L. Thijs, J. Van Humbeeck, J. Kruth, Mater. Sci. Technol. **31** (2014)
16. K.P. Monroy, J. Delgado, L. Sereno, J. Ciurana, N.J. Hendrichs, Met. Mater. Int. **20** (2014)
17. X. Tong, F.-h. Li, M. Liu, M.-j. Dai, H. Zhou, Opt. Laser Technol. **42** (2010)
18. M. Aghasibeig, H. Fredriksson, Surf. Coat. Technol. **209** (2012)
19. I. Hemmati, R.M. Huizenga, V. Ocelík, J.Th.M. De Hosson, Acta Mater. **61** (2013)

20. E. Feldshtein, M. Kardapolava, O. Dyachenko, Surf. Coat. Technol. **307** (2016)
21. G.M. Krolczyk, P. Nieslony, J.B. Krolczyk, I. Samardzic, S. Legutko, S. Hloch, S. Barrans, R.W. Maruda, Measurement **70** (2015)
22. L. Janka, J. Norpoth, S. Eicher, M.R. Ripoll, P. Vuoristo, Mater. Des. **98** (2016)